Electronic Supplementary Material (ESI) for Catalysis Science & Technology.

In-situ modulation of silica-supported MoO_2/Mo_2C heterojunction for enhanced hydrogen evolution reaction

Rajinder Kumar,[a] Zubair Ahmed,[a] Ravi Kumar,[b] [a] Shambhu Nath Jha,[b] Dibyendu Bhattacharyya,[b] Chandan Bera, * and Vivek Bagchi [a] *

[a] *Institute of Nano Science and Technology, Phase-10, Sector-64, Mohali, Punjab 160062, India*

[b] *Atomic and Molecular Physics Division Bhabha Atomic Research Centre, Mumbai- 400 085*

Supporting information

List of Content

S1. Detailed information of catalyst synthesis

The synthesis of all the catalysts were carried out in two major steps. First, the preparation of metal precursor and second, the calcination of the molybdenum precursor by temperatures controlled annealing in an argon atmosphere at different time periods.

a. **Synthesis of MoO_3 nanoparticles**: For the hydrothermal synthesis of MoO_3 nanoparticles, two separate solutions containing ammonium molybdate (0.001 moles, 1.2358 gm) and citric acid (0.03 moles, 5.8 gm) were prepared by dissolving each in 20 mL of distilled water. A few drops of 12 M HCl were added to the obtained transparent solution by stirring to maintain a pH of 1-2 resulting in a blue coloured solution. This bluish-coloured solution heated at 180 °C for the next 24 h in a hydrothermal bomb. The obtained hydrothermal product was dried at 100 °C. Finally, the powder was heated at 500 °C for 2 h to yield MoO_3 nanoparticles.

b. **MoO_2:** MoO_2 catalyst was synthesized by annealing 15 mg of MoO_3 with 100 mg of GO-based carbon source (preparation described in the experimental section of the manuscript) at 800 °C for 1 h in an argon atmosphere at a flow rate of 30 mL/min.

c. **Mo_2C:** For Mo_2C catalyst has been synthesized with 15 mg MoO_3 nanoparticles and 250 mg GO-based carbon source, mixed in a mortar pestle. The mixture was heated at 800 °C for 3 h in argon atmosphere with a flow rate of 30 mL/min.

d. **Silica-based MoO_2 (Si-MoO_2):** Si-MoO_2 was synthesized by annealing 25 mg of Si-MoO_3 (as mentioned in manuscript) with 100 mg of GO-based carbon source annealed at 800 °C for 1 h in an argon atmosphere at a flow rate of 30 mL/min.

e. **Silica-based Mo_2C (Si-Mo_2C):** Si-Mo_2C catalyst was synthesized annealing 25 mg Si-MoO_3 nanoparticles (preparation described in the experimental section of the manuscript) and 250 mg GO based carbon source was mixed in a mortar pestle. The mixture was heated at 800 °C for 3 h in an argon atmosphere with a flow rate of 30 mL/min.

f. **SiMoCat1:** SiMoCat1 was synthesized by annealing a mixture of 25 mg Si-MoO_3 precursor (as mentioned in the manuscript) and 225 mg of GO-based carbon source for 3.5 h at 800 °C in argon atmosphere.

g. **SiMoCat2:** SiMoCat2 was synthesized by annealing a mixture of 25 mg Si-MoO_3 precursor (as mentioned in the manuscript) and 100 mg of GO-based carbon source for 2.5 h at 800 °C in argon atmosphere.

Note: The heating rate in all the synthesis process was 400 °C/min, and the post-reaction cooling was done in an argon environment with a gas flow of 30 mL/min.

S2.1. PXRD and DLS study of Si-MoO_3 nanoparticles

The XRD pattern was obtained in the 2θ angular region of 5° to 80° with an increment of 0.00190/Step. DLS measurements were performed on Malvern zetasizer nano ZSP instrument.

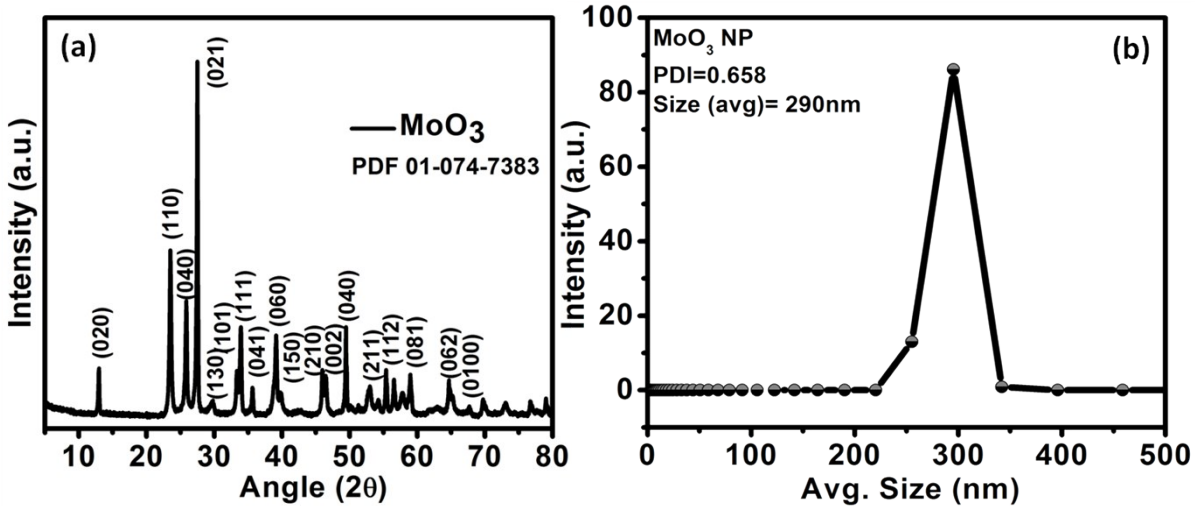

Figure S1. PXRD (a) and DLS (b) pattern of Si-MoO_3 nanoparticles

S2.2. PXRD pattern of GO based precursor (Melamine-GO)

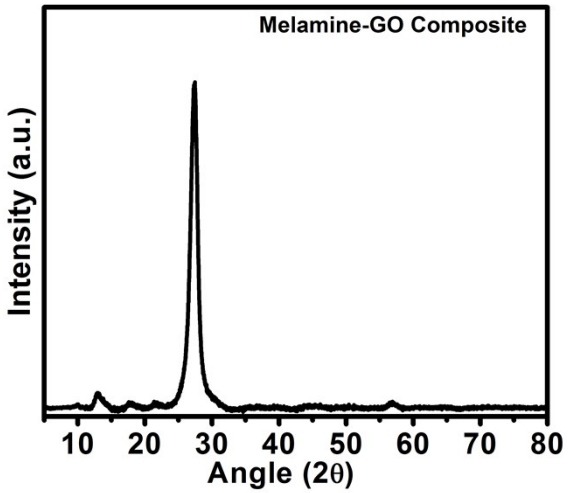

Figure S2. PXRD pattern of Melamine-GO Composite

S2.3. PXRD pattern of Si-Mo_2C and Si-MoO_2

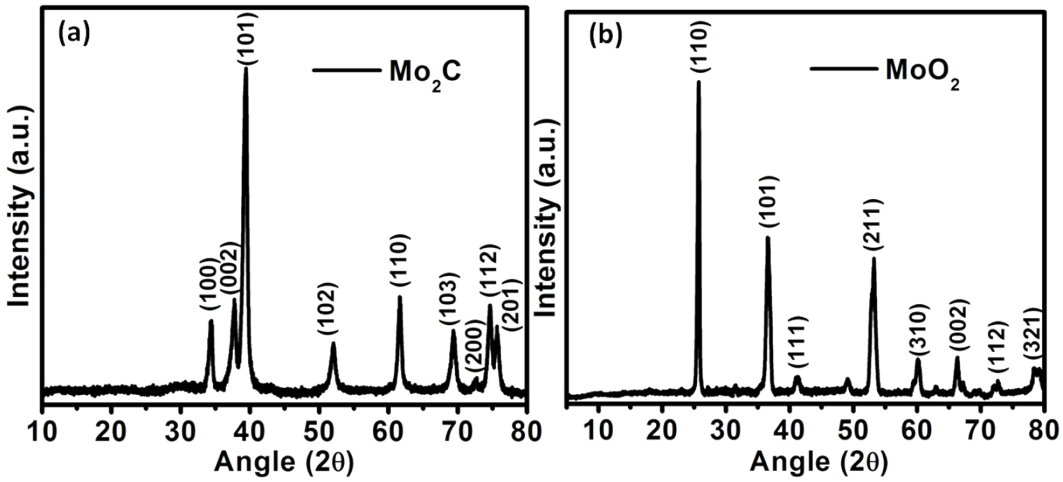

Figure S3. PXRD of (a) Si-Mo_2C and (b) Si-MoO_2

S3.1. Rietveld refinement study of SiMoCat1 and SiMoCat2

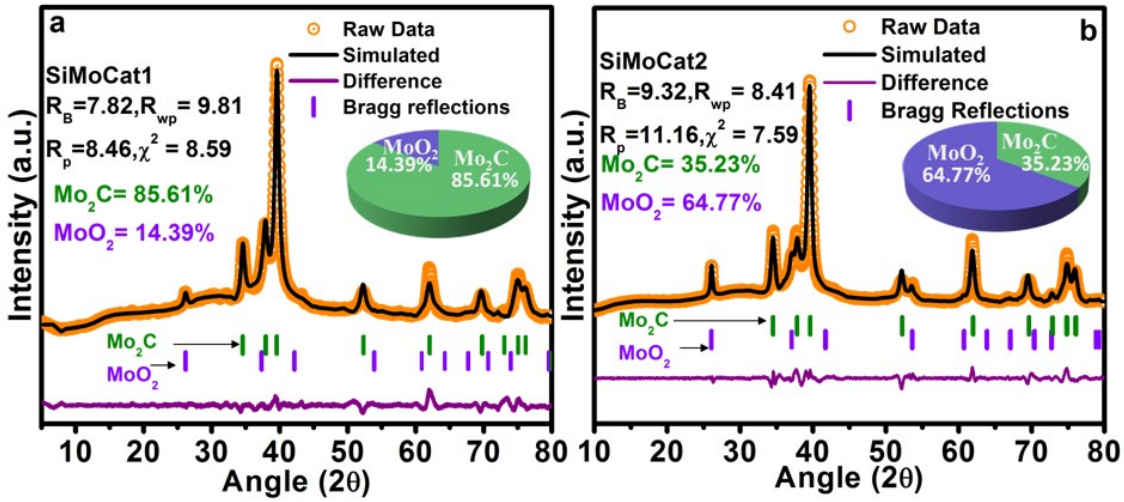

Figure S4. Rietveld refinement of (a) SiMoCat1 and (b) SiMoCat2: The figure typically shows formation of both Mo_2C and MoO_2 phases and Rietveld analysis of catalyst shows a composition 85.61 % and 14.39 % of Mo_2C and MoO_2 respectively in SiMoCat1 and a composition of 35.23 % and 64.77 % of Mo_2C and MoO_2 respectively in SiMoCat2.

S3.2. Rietveld refinement parameters of the catalysts

Tables (below) showing the unit cell parameters of SiMoCat, SiMoCat1, and SiMoCat2 and their corresponding refinement values

SiMoCat

Sr. No.	Parameters	Mo_2C		MoO_2	
1	Symmetry	Hexagonal		Tetragonal	
2	Space group	194		136	
		Input	Output	Input	Output
3	a	2.99091 Å	2.98920 Å	4.82993 Å	4.83969 Å
4	b	2.99091 Å	2.98920 Å	4.82993 Å	4.83969 Å
5	c	4.71022 Å	4.75052 Å	2.81968 Å	2.78542 Å
6	α	90^0	90^0	90^0	90^0
7	β	90^0	90^0	90^0	90^0
8	γ	120^0	120^0	90^0	90^0
9	R_p %	10.36			
10	R_{wp} %	9.31			
11	χ^2	4.59			

Table S1. Refinement parameters of SiMoCat

SiMoCat1

Sr. No.	Parameters	Mo_2C		MoO_2	
1	Symmetry	Hexagonal		Tetragonal	
2	Space group	194		136	
		Input	Output	Input	Output
3	a	2.99091 Å	2.99376 Å	4.82993 Å	4.81431 Å
4	b	2.99091 Å	2.99376 Å	4.82993 Å	4.81431 Å
5	c	4.71022 Å	4.74662 Å	2.81968 Å	2.76749 Å
6	α	90^0	90^0	90^0	90^0
7	β	90^0	90^0	90^0	90^0
8	γ	120^0	120^0	90^0	90^0
9	R_p %	8.46			
10	R_{wp} %	9.81			
11	χ^2	8.59			

Table S2. Refinement parameters of SiMoCat1

SiMoCat2

Sr. No.	Parameters	Mo_2C		MoO_2	
1	Symmetry	Hexagonal		Tetragonal	
2	Space group	194		136	
		Input	Output	Input	Output
3	a	2.99091 Å	2.99696 Å	4.82993 Å	4.83366 Å
4	b	2.99091 Å	2.99696 Å	4.82993 Å	4.83666 Å
5	c	4.71022 Å	4.75537 Å	2.81968 Å	2.80616 Å
6	α	90^0	90^0	90^0	90^0
7	β	90^0	90^0	90^0	90^0
8	γ	120^0	120^0	90^0	90^0
9	R_p%	11.16			
10	R_{wp}%	8.41			
11	χ^2	7.59			

Table S3. Refinement parameters of SiMoCat2

S4.1. XANES and EXAFS studies:

The XAFS measurements of the Mo based catalysts along with the Mo standards have been carried out at the Energy Scanning EXAFS beamline (BL-9) at the Indus-2 Synchrotron Source (2.5 GeV, 100 mA), Raja Ramanna Centre for Advanced Technology (RRCAT), Indore, India[1-2] on Mo K-edges. This beamline operates in the energy range of 4 KeV to 25 KeV. The beamline optics consists of a Rh/Pt coated collimating meridional cylindrical mirror and the collimated beam reflected by the mirror is monochromatized by a Si (111) (2d=6.2709 Å) based double crystal monochromator (DCM). The second crystal of DCM is a sagittal cylinder used for horizontal focusing while Rh/Pt coated bendable post mirror facing down is used for vertical focusing of the beam at the sample position. Rejection of the higher harmonics content in the X-ray beam is performed by detuning the second crystal of DCM. In the present case, XAS measurements have been performed in both transmission and fluorescent modes. For the transmission mode measurement, three ionization chambers (300 mm length each) have been used for data collection, one ionization chamber for measuring incident flux (I_0), the second one for measuring transmitted flux (I_t) and the third ionization chamber for measuring XAS spectrum of a reference metal foil for energy calibration. Appropriate gas pressure and gas mixtures have been chosen to achieve 10-20% absorption in the first ionization chamber and 70-90% absorption in the second ionization

chamber to improve the signal to noise ratio. The absorption coefficient μ is obtained using the relation:

$$I_T = I_0 e^{-\mu x} \quad (1)$$

where x is the thickness of the absorber.

For measurements in the fluorescence mode, the sample is placed at 45° to the incident X-ray beam and a fluorescence detector is placed at a right angle to the incident X-ray beam to collect the signal. One ionization chamber detector is placed prior to the sample to measure the incident flux (I_0) and fluorescence detector measures the fluorescence intensity (I_f). From these intensities, the absorbance of the sample ($\mu = I_f / I_0$) is found as a function of energy.

Mo edge:

The Mo K-edge absorption edges of the samples have been obtained from the 1st inflexion point of the μ vs. E curves. The K-edge energy in XANES and Fourier transformed EXAFS (FT-EXAFS) of Mo precursor, Mo foil along with the references MoO_2 and Mo_2C as reference sample are studied to compare with the SiMoCat catalyst. From the XANES spectrum, it can be seen that the oxidation state of the sample is less than +6. The absorption edges of Mo in the samples SiMoCat lies very close to the Mo_2C towards to low energy side of MoO_2, which shows that Mo in SiMoCat having an oxidation in between 2 and 3 with little energy difference form the Mo_2C energy edge value. The XANES spectrum of AMH ($(NH_4)_6Mo_7O_{24}$) shows pre-edge at 20007 eV which is due to 1s-4d dipole forbidden transition. AMH has tetrahedral symmetry, which has mixed Mo-d and O-p bond characters.

To obtain the qualitative information about the local structure, oscillations in the absorption spectra $\mu(E)$ have been converted to absorption function $\chi(E)$ defined as follows:

$$\chi(E) = \frac{\mu(E) - \mu_0(E)}{\Delta\mu_0(E_0)} \quad (2)$$

where E_0 is the absorption edge energy, $\mu_0(E_0)$ is the bare atom background and $\Delta\mu_0(E_0)$ is the step in $\mu(E)$ value at the absorption edge. The energy-dependent absorption coefficient $\chi(E)$ has been converted to the wave-number dependent absorption coefficient $\chi(k)$ using the relation,

$$K = \sqrt{\frac{2m(E - E_0)}{\mathrm{h}^2}} \qquad (3)$$

where m is the electron mass. $\chi(k)$ is weighted by k^2 to amplify the oscillation at high k and the $\chi(k)k^2$ functions are Fourier transformed in R space to generate the $\chi(R)$ versus R spectra in terms of the real distances from the centre of the absorbing atom. The set of EXAFS data analysis programme available within Demeter[3] software package has been used for EXAFS data analysis. This includes background reduction and Fourier transforms to derive the $\chi(R)$ versus R spectra from the absorption spectra (using ATHENA[3] software), generation of the theoretical EXAFS spectra starting from an assumed crystallographic structure and finally fitting of experimental data with the theoretical spectra using ARTEMIS[3] software. To obtain the qualitative information about the local structure, oscillations in the absorption spectra $\mu(E)$ have been converted to absorption function $\chi(E)$ defined as follows:

$$\chi(E) = \frac{\mu(E) - \mu_0(E)}{\Delta\mu_0(E_0)} \qquad (4)$$

where E_0 is absorption edge energy, $\mu_0(E_0)$ is the bare atom background and $\Delta\mu_0(E_0)$ is the step in $\mu(E)$ value at the absorption edge. The energy-dependent absorption coefficient $\chi(E)$ has been converted to the wavenumber dependent absorption coefficient $\chi(k)$ using the relation,

$$K = \sqrt{\frac{2m(E - E_0)}{\mathrm{h}^2}} \qquad (5)$$

where m is the electron mass. $\chi(k)$ is weighted by k^2 to amplify the oscillation at high k and the $\chi(k)k^2$ functions are Fourier transformed in R space to generate the $\chi(R)$ versus R spectra in terms of the real distances from the centre of the absorbing atom. The set of EXAFS data analysis programme available within Demeter[3] software package has been used for EXAFS data analysis. This includes background reduction and Fourier transforms to derive the $\chi(R)$ versus R spectra from the absorption spectra (using ATHENA[3] software), generation of the theoretical EXAFS spectra starting from an assumed crystallographic structure and finally fitting of experimental data with the theoretical spectra using ARTEMIS[3] software. The $\chi(R)$ versus R plots at Mo K-edges

are shown in figure S7 for the catalyst SiMoCat. The data of these samples have been fitted by taking Mo_2C and MoO_2 crystal structure. In the fitting process the co-ordination number (C.N), atom to atom bond distance (R) between the respective atomic pairs and the disorder factor (Debye-Waller factor) (σ^2), which gives the mean square fluctuation in the atomic bond lengths and the thermal disorder in the system, have been used as fitting parameters and the best-fit parameters have been shown in table S4. The goodness of fit has been determined by the value of the R_{factor} defined by:

$$R_{factor} = \sum \frac{[\mathrm{Im}(\chi_{dat}(r_i) - \chi_{th}(r_i)]^2 + [\mathrm{Re}(\chi_{dat}(r_i) - \chi_{th}(r_i)]^2}{[\mathrm{Im}(\chi_{dat}(r_i)]^2 + [\mathrm{Re}(\chi_{dat}(r_i)]^2} \qquad (6)$$

where, χ_{dat} and χ_{th} refer to the experimental and theoretical $\chi(r)$ values respectively and Im and Re refer to the imaginary and real parts of the respective quantities. From figure S7 it can be seen that SiMoCat have a radial distribution which basically is a linear combination of MoO_2 and Mo_2C radial distribution. The first and second peak has the contribution of Mo-O and Mo-C coordination shell, while the third peak has the contribution of Mo-Mo coordination shell. The best-fit parameters have been shown in Section S4.3, Table S4.

S4.2. EXAFS measurments of standard MoO_2, Mo_2C, and SiMoCat

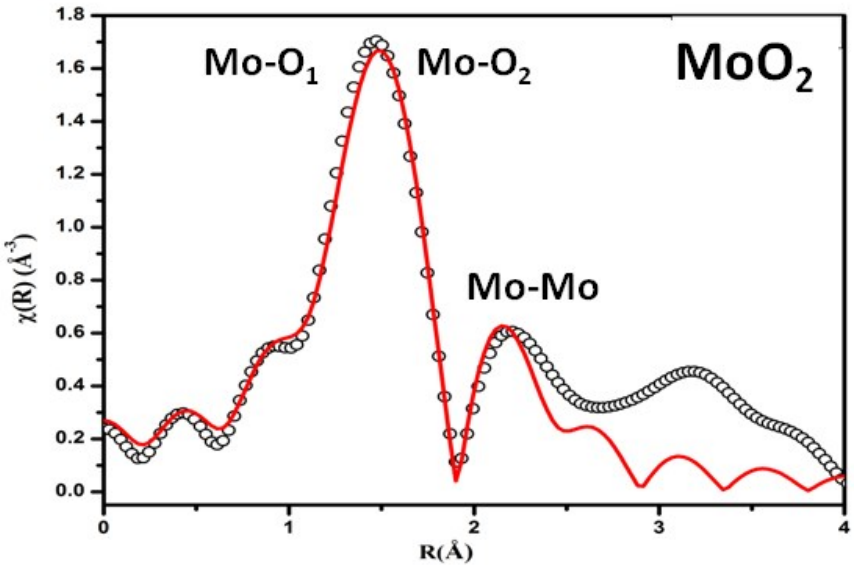

Figure S5. Fourier transformed EXAFS spectrum of MoO_2 sample measured at Mo K-edge along with best-fit theoretical spectrum. The experimental spectrum is represented by scatter points and the theoretical fit is represented by solid line.

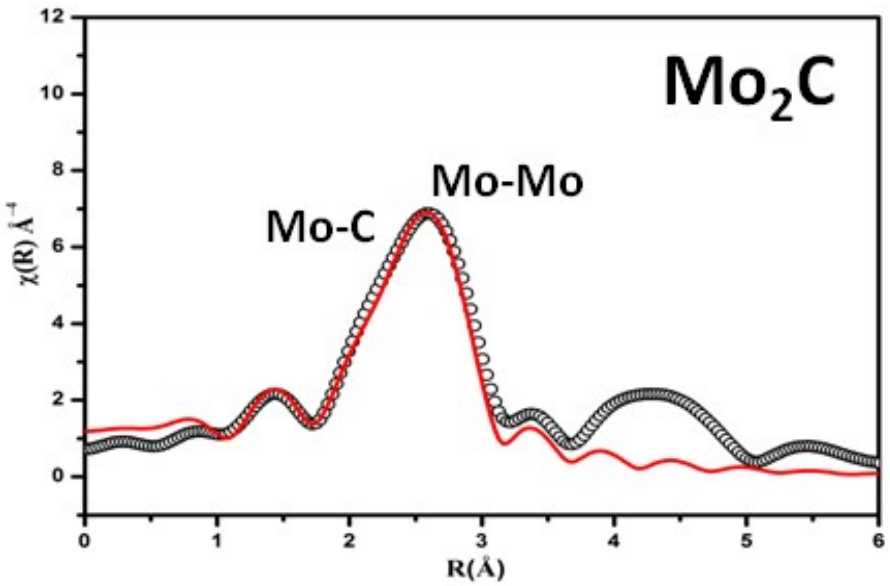

Figure S6. Fourier transformed EXAFS spectrum of Mo_2C sample measured at Mo K-edge along with best-fit theoretical spectrum. The experimental spectrum is represented by scatter points and the theoretical fit is represented by a solid line.

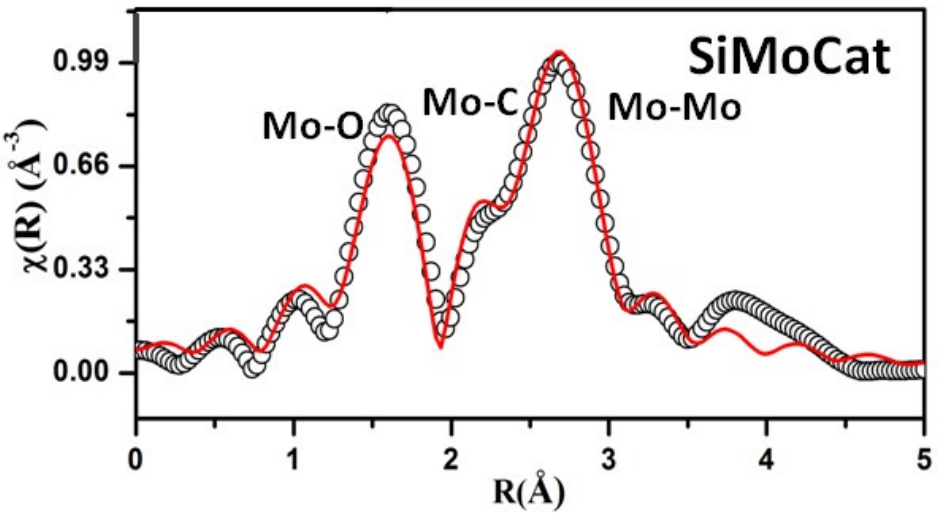

Figure S7. Fourier transformed EXAFS spectrum of SiMoCat sample measured at Mo K-edge along with best-fit theoretical spectrum. The experimental spectrum is represented by scatter points and the theoretical fit is represented by a solid line.

S4.3. Table for Bond length, coordination number and disorder factor obtained from EXAFS fitting for the samples SiMoCat at Mo K-edge

Path	Parameter	SiMoCat	Path	Parameter	MoO_2	Path	Parameters	Mo_2C
Mo edge			Mo edge			Mo edge		
Mo-C (From Mo_2C)	R (Å) (2.09)	2.14 ± 0.01	$Mo-O_1$	R (Å) (1.98)	1.98 ± 0.002	Mo-C	R (Å) (2.09)	2.14 ± 0.04
	N(6)	6.0 ± 0.12		N(4)	4.0 ± 0.05		N(6)	5.53 ± 1.26
	σ^2	0.001		σ^2	0.0015 ± 0.0004		σ^2	0.024 ± 0.009
Mo-Mo (From Mo_2C)	R (Å) (2.99)	2.96 ± 0.003	$Mo-O_2$	R (Å) (2.07)	2.07 ± 0.003	Mo-Mo	R (Å) (2.99)	2.93 ± 0.01
	N(6)	6.0 ± 0.12		N(2)	2.0 ± 0.03		N(12)	11.46 ± 1.68
	σ^2	0.002 ± 0.0006		σ^2	0.0015 ± 0.0004		σ^2	0.011 ± 0.001
$Mo-O_1$ (From MoO_2)	R (Å) (1.98)	1.83 ± 0.002	Mo-Mo	R (Å) (2.51)	2.59 ± 0.006			
	N(4)	4.0 ± 0.07		N(1)	1.0 ± 0.01			
	σ^2	0.045 ± 0.007		σ^2	0.0013 ± 0.0003			
$Mo-O_2$ (From MoO_2)	R (Å) (2.07)	1.91 ± 0.003						
	N(2)	2.0 ± 0.05						
	σ^2	0.045 ± 0.007						
R_{factor}		0.01	R_{factor}		0.02	R_{factor}		0.001

Table S4. Bond length, coordination number and disorder factor obtain by EXAFS fitting for the samples SiMoCat at Mo K-edge

S5. STEM analysis of SiMoCat

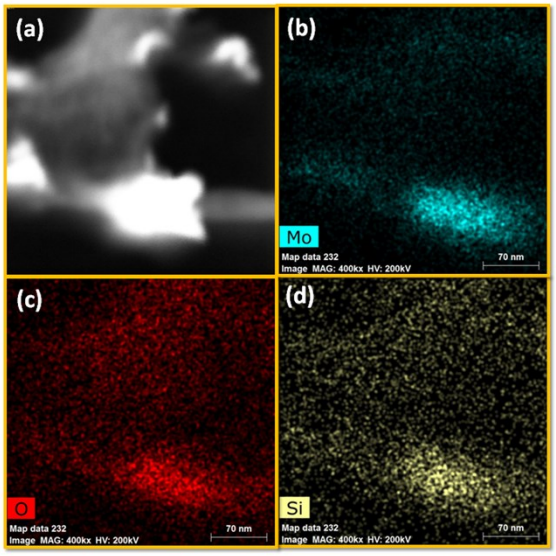

Figure S8. STEM images of SiMoCat Catalyst: The images showing the presence of Mo, O and Si in the SiMoCat

S6. BET analysis of Si-MoO_3 and SiMoCat

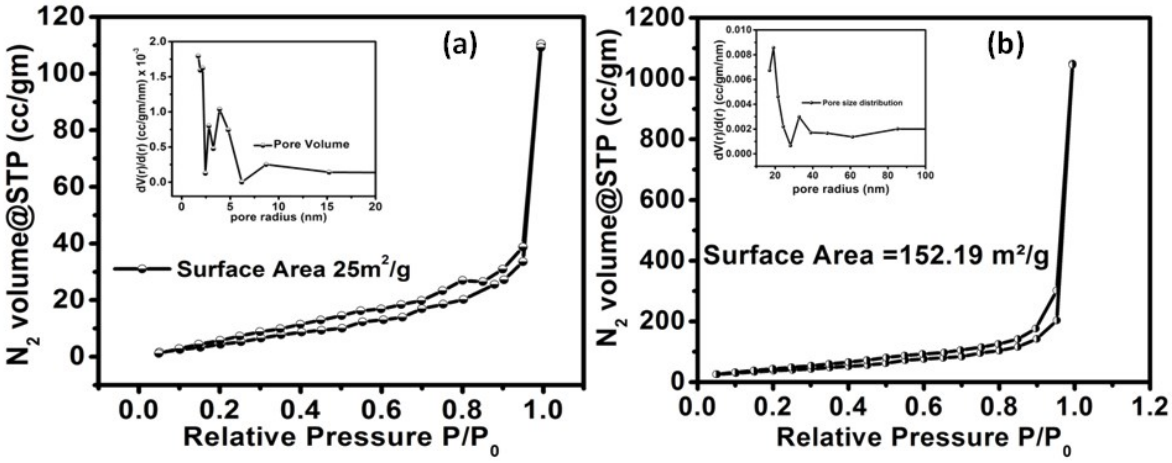

Figure S9. Nitrogen adsorption BET isotherms and inset showing BJH pore distribution of the catalyst (a) Si-MoO_3 (b) SiMoCat: The catalyst was degassed at temperature 200 ^{0}C for 6 h before BET analysis

S7.1. Polarisation curves of other synthesized electrocatalysts

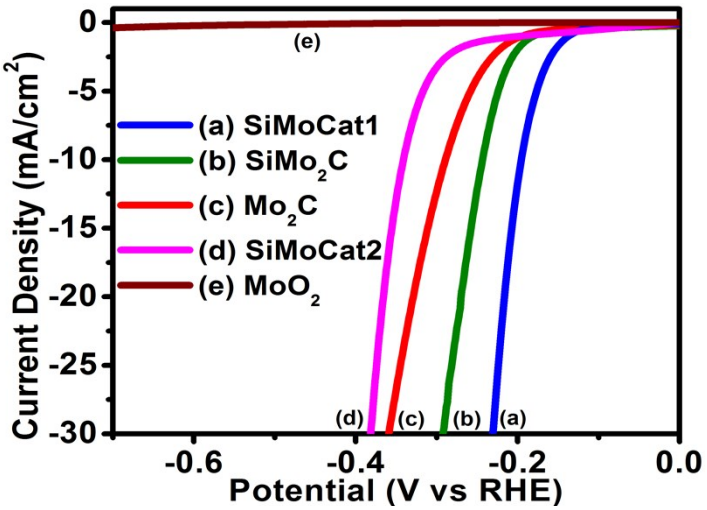

Figure S10. Polarisation curve of catalyst (a) SiMoCat1 (b) Si-Mo_2C (c) Mo_2C (d) SiMoCat2 (e) MoO_2 in 0.5 M acidic media

S7.2. A comparision of kinetic parameters of all the catalysts

Catalyst	Onset (vs RHE)	η_{10} (vs RHE)	η_{20} (vs RHE)	η_{30} (vs RHE)	Tafel Slope (mV/dec)	Exchange Current Density (mA/cm^2)
SiMoCat	31 mV	71 mV	86 mV	90 mV	35	2.33×10^{-2}
Mo_2C	204 mV	290 mV	328 mV	359 mV	97	5.71×10^{-3}
SiMo_2C	187 mV	244 mV	271 mV	293 mV	85	6.32×10^{-3}
SiMoCat1	137 mV	195 mV	216 mV	229 mV	62	8.16×10^{-3}
SiMoCat2	218 mV	342 mV	349 mV	380 mV	112	1.39×10^{-4}
SiMoCat-m	209 mV	285 mV	311 mV	329 mV	82	4.17×10^{-3}

Table S5. Calculated kinetic parametrs of different catalyst in 0.5 M H_2SO_4 solution

S7.3. EIS measurements of SiMoCat and SiMoCat-m.

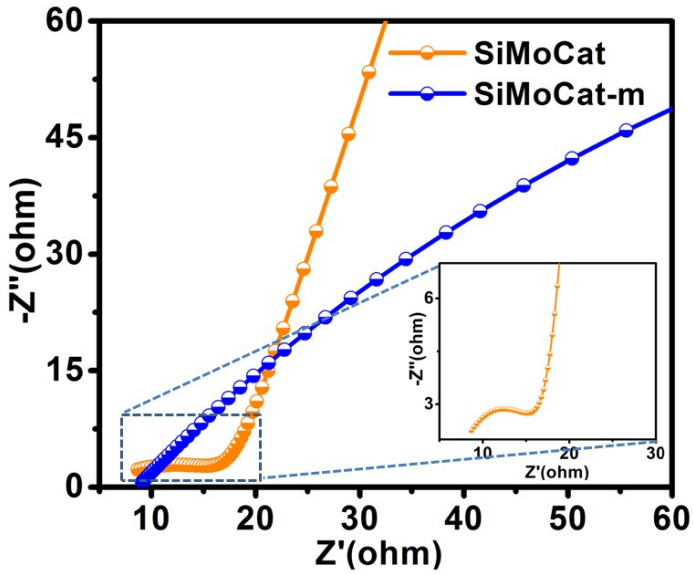

Figure S11. Nyquist plot of SiMoCat and SiMoCat-m; Inset: magnified image of SiMoCat catalyst at 50 mV applied potential.

S8. Theoretical Study

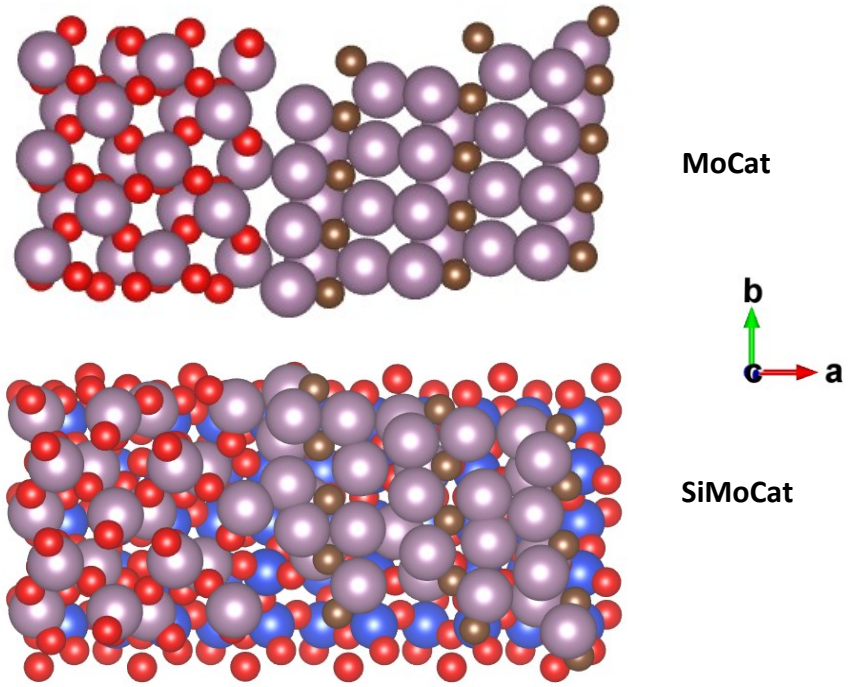

Figure S12. (Top) Heterostructure of Mo_2C and MoO_2 . (Bottom) Mo_2C and MoO_2 heterostructure on SiO_2 substarte. <101> surface exposed for Hydrogen absorption.

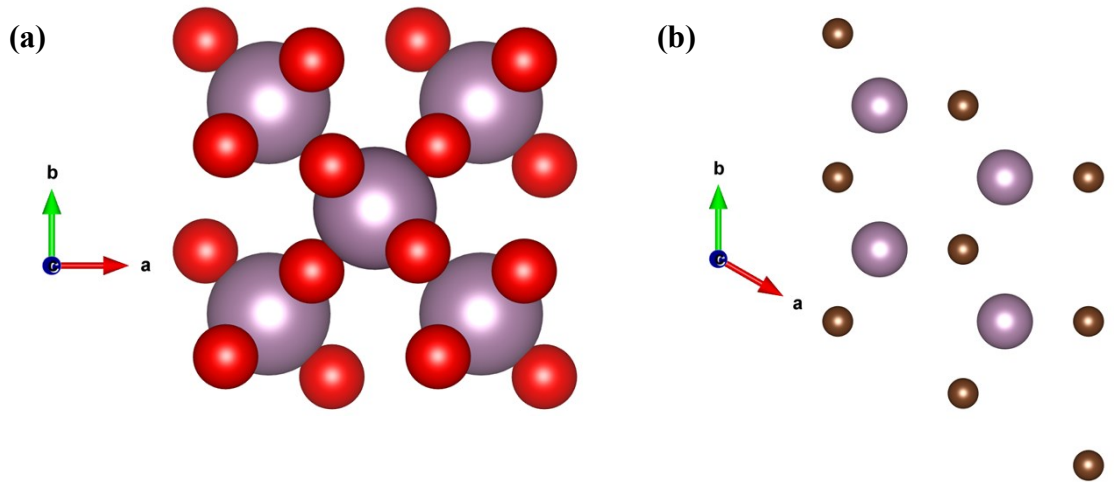

Figure S13. (a) Tetragonal MoO_2 with lattice constant a= 4.8 Å, b= 4.8 Å and c= 3.2Å, (b) Hexagonal Mo_2C with lattice constant a= 2.88 Å, b= 2.88 Å and c= 5.48Å.

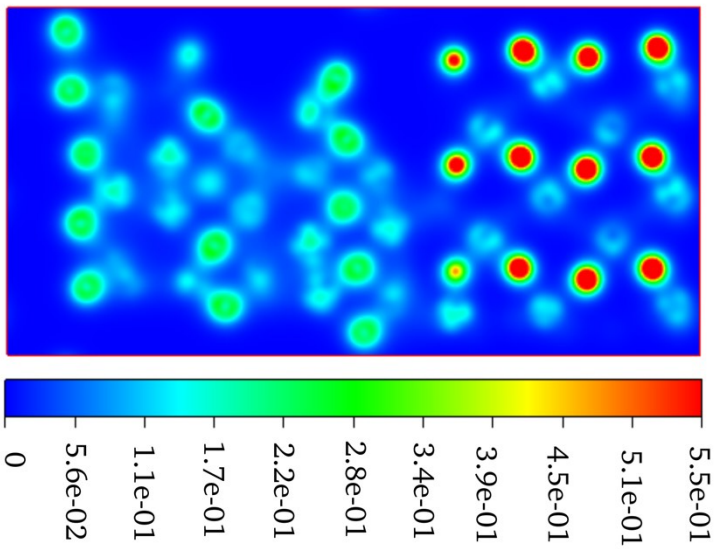

Figure S14. Surface charge distribution on SiMoCat <101> plane. It is found that charge density is very high around Mo atoms which make strong M-H bond and attract lot of hydrogen to surface. Comparatively O atoms have less and C atoms have very less charge density.

References

1. Poswal, A. K.; Agrawal, A.; Yadav, A. K.; Nayak, C.; Basu, S.; Kane, S. R.; Garg, C. K.; Bhattachryya, D.; Jha, S. N.; Sahoo, N. K., Commissioning and first results of scanning type EXAFS beamline (BL-09) at INDUS-2 synchrotron source. *AIP Conference Proceedings* 2014, *1591* (1), 649-651.
2. Basu, S.; Nayak, C.; Yadav, A. K.; Agrawal, A.; Poswal, A. K.; Bhattacharyya, D.; Jha, S. N.; Sahoo, N. K., A comprehensive facility for EXAFS measurements at the INDUS-2 synchrotron source at RRCAT, Indore, India. *Journal of Physics: Conference Series* 2014, *493* (1), 012032.
3. Newville, M.; Ravel, B.; Haskel, D.; Rehr, J. J.; Stern, E. A.; Yacoby, Y., Analysis of multiple-scattering XAFS data using theoretical standards. *Physica B: Condensed Matter* 1995, *208-209*, 154-156.